Evaluation of Ionic Mobilities by Coupling the Scattering on Atoms and on Electron Density

Alexandre A. Shvartsburg,[†] Bei Liu,[‡] K. W. Michael Siu,*[,†] and Kai-Ming Ho[‡]

Department of Chemistry, York University, 4700 Keele Street, Toronto, Ontario, Canada M3J 1P3, and Ames Laboratory and Department of Physics and Astronomy, Iowa State University, Ames, Iowa 50011

Received: February 7, 2000; In Final Form: April 12, 2000

A recently developed method to calculate gas-phase mobilities by scattering on electron density isosurfaces (SEDI) has been applied to carbon cluster ions. The investigation has covered species belonging to all major structural families identified in drift tube studies (chains, monocyclic and bicyclic rings, graphite sheets, and fullerenes). Relative cross sections of C_n^- and C_n^+ predicted by SEDI are in excellent agreement with the measurements across a wide range of cluster sizes and shapes. However, absolute values could not be fit for either charge state. This happens because SEDI ignores the long-range ion−buffer gas interaction known to be important for many systems including carbon clusters. To overcome this problem, we propose a new technique to evaluate mobilities by coupling SEDI with trajectory calculations. This approach allows one to introduce the repulsive interaction accurately and still account for the attractive part of the potential. This hybrid SEDI−TC treatment has been found substantially superior to all models previously described in reproducing both absolute and relative mobilities of C_n anions and cations.

I. Introduction

Over the past decade, ion mobility spectrometry (IMS) has been established as a powerful, widely applicable tool to characterize the geometries of gas-phase ions. The technique is based on the fact that isomers of differing shapes travel with unequal velocities when drifting through a gas pulled by an electric field, and thus can be separated from each other.[1] The resolved peaks are assigned by comparing the measured mobilities with values computed for plausible candidate geometries. Hence the analysis of experimental data depends critically on the accuracy of mobility calculations. This has been particularly true since high-resolution measurements in the IMS/MS configuration[2] enhanced the resolving power by an order of magnitude over the capability of MS/IMS/MS injected drift tube instruments.[3] Matching the presently achieved experimental resolution of <1% by a similar precision of mobility calculations is an immense theoretical challenge.

Mobility measurements are normally performed in the low drift field regime, where the directional velocity of ions is negligible compared to the thermal velocity of buffer gas atoms and is therefore proportional to the drift field intensity. Further, when the buffer gas atoms are much lighter than the drifting ion (Rayleigh limit), the evaluation of mobility reduces to determination of the first-order orientationally averaged collision integral,[4,5] $\Omega_{avg}^{(1,1)}$

$$K = \frac{(18\pi)^{1/2}}{16}\left[\frac{1}{m} + \frac{1}{m_B}\right]^{1/2} \frac{ze}{(k_B T)^{1/2}} \frac{1}{\Omega_{avg}^{(1,1)}} \frac{1}{N} \qquad (1)$$

Here m and m_B are, respectively, the masses of the ion and of the buffer gas atom, N is the buffer gas number density, ze is the ionic charge, and T is the effective gas temperature. The earliest method to calculate $\Omega_{avg}^{(1,1)}$ (below simply Ω) for an arbitrary ion is the "projection approximation" dating back[6] to 1925. In this model, the collision integral is equated to the hard-sphere projection. This approach has originally been designed by Mack[6] to evaluate the diffusion constants of neutral molecules in gases. Remarkably, this was until very recently the only formalism for computing the cross section of a polyatomic ion[2,7,8] (in the zero-field limit this quantity is inversely proportional to the diffusion constant[4]). Projection approximation has been shown to yield grossly inaccurate mobilities for many objects. This is always the case for ions with concave surface areas such as fullerene dimers and oligomers.[9,10] However, large errors are often encountered also for objects that are convex overall. For example, experimental drift times for carbon chain cations have been found[7,8] to deviate from expected values by more than 10%. Due to errors of this magnitude, the use of projection approximation causes wrong structural assignments for a number of systems.[9−12]

Once the drastic improvement in experimental resolution[3] had clearly shifted the emphasis in extending the frontier of IMS toward data analysis, the development of more accurate methods for mobility calculations became topical. Rigorously, Ω should be evaluated by integrating the momentum transfer cross section over the Maxwellian distribution of relative velocities (at the temperature T) between the buffer gas atom and the ion. This cross section is determined by averaging a function of the scattering angle χ over the impact parameter b and the collision geometry defined by angles θ, φ, and γ:

$$\Omega = \frac{1}{8\pi^2}\int_0^{2\pi} d\theta \int_0^{\pi} d\varphi \times \sin\varphi \int_0^{2\pi} d\gamma \frac{\pi}{8}\left[\frac{\mu}{k_B T}\right]^3 \int_0^{\infty} dg \times e^{-\mu g^2/(2k_B T)} g^5 \int_0^{\infty} 2b\, db\, (1 - \cos\chi(\theta,\varphi,\gamma,g,b)) \qquad (2)$$

[†] York University.
[‡] Iowa State University.

10.1021/jp0004765 CCC: $19.00
Published on Web 06/10/2000

where μ is the reduced mass of the ion and buffer gas atom and g is their relative velocity. Equation 2 has been solved[13] numerically via classical trajectory calculations, assuming elastic collisions with rigid irrotational ions. These calculations employed a potential consisting of pairwise Lennard-Jones interactions between the buffer gas atom and each atom in the cluster plus a charge−induced dipole term incorporating arbitrary partial charges on all cluster atoms. In practice, two parameters of the elementary LJ potential (ϵ, the depth, and σ, the distance where $\epsilon = 0$) are fit to reproduce the mobility of an ion with known geometry as a function of buffer gas temperature.[13] For example, measurements for C_{60}^+ fullerene are best fit[13] by $\epsilon_{C-He} = 1.34$ meV and $\sigma_{C-He} = 3.043$ Å. The exact hard-spheres scattering (EHSS) model[14] is a special case of trajectory calculations with the LJ potentials centered on all cluster atoms replaced by vertical wall potentials. Trajectory calculations and EHSS have been proven consistently superior to the projection approximation in reproducing the measured mobilities, including those for clusters of carbon,[9−11,13,15] silicon,[12] germanium,[16] and salt,[17,18] as well as biomolecular ions.[19,20]

Yet in certain cases even the mobilities resulting from trajectory calculations deviate from the measured values noticeably. For example, the collision integrals of C_n^+ chains are overestimated[11] by up to 8%. This is significantly better than the error of ∼20% produced by the projection approximation,[11] but further improvement is warranted considering the experimental accuracy of ∼1%. However, the main problem appears to be modeling the mobilities of negatively charged clusters. For some time IMS work had been undertaken for cations only, and only recently a few studies for anions appeared.[9−11,15,17,21−26] It is now clear that the cross sections for anions typically exceed those for respective cations substantially. The sign of ionic charge is obviously immaterial for either the projection approximation or trajectory calculations in additive pairwise LJ potentials[11,13] (including EHSS[14]); hence the difference in mobilities between cations and anions is not reconcilable with those methods. More importantly, the mobilities for Si_n^- could not be reproduced by trajectory calculations even if the model parameters are fit for an anion.[27]

Physically, the buffer gas atoms are scattered on the electronic clouds of ions, and obviously the cross sections for anions are greater than those for cations because the addition of two electrons expands these clouds. This suggests that further improvements in mobility calculations are attainable by involving some information about the electronic orbitals of drifting ion rather than only its nuclear geometry, as is the case with all approaches described above. The first step in this direction has been the scattering on electron density isosurfaces (SEDI) model.[27] In this treatment, the buffer gas atoms are scattered on the electronic cloud represented by a surface where the electron density, E_{cut}, assumes a certain value. Analogous to the approach used with trajectory calculations and EHSS, the quantity E_{cut} is adjusted to fit the measurement for one ion with a known geometry and then transferred to other species. This method has been tested for Si_n anions ($n \leq 20$) drifting in He and produced an excellent agreement with experiment.[27]

While SEDI is evidently superior to EHSS in describing the repulsive part of the ion−buffer gas potential, both models ignore the attractive interaction. SEDI has still performed well for Si_n ions because the magnitude of that interaction is nearly independent of the cluster size and shape.[27] This is due to large Si−Si bond lengths ($L \sim 2.5$ Å), which prevents an effective interaction of buffer gas atom with more than several cluster atoms at once. Thus SEDI has been expected[27] to be adequate for species with large bond lengths, such as Ge_n and Sn_n ions, but not C_n with $L \sim 1.3$ Å where the overall depth of molecular interaction potential depends on cluster geometry strongly.[11] In this contribution, we investigate the performance of SEDI model for C_n cations and anions, and prove it unacceptable as anticipated. Further, we lay out a new SEDI/trajectory calculations hybrid method that should be suitable for all kinds of ions, and demonstrate its validity for carbon species.

II. Mobilities for C_n Ions Calculated Using SEDI

Molecular electronic orbitals have, in general, irregular shapes. Therefore, a surface of equal electron density has to be defined numerically as a set of points in space. The hard-sphere collision integral for the body thus obtained is calculated employing an algorithm resembling EHSS[14] that implements the equation

$$\Omega = \frac{1}{4\pi}\int_0^{2\pi} d\theta \int_0^{\pi} d\varphi \times \sin\varphi \int_0^{2\pi} d\gamma \int_0^{\infty} b\, db(1 - \cos\chi(\theta,\varphi,\gamma,b)) \quad (3)$$

Technically, the points comprising a surface are located on a three-dimensional grid of variable periodicity.[27] The mesh is made finer until Ω converges. A surface is obviously better delineated by a finer grid, but this has to be balanced against the computational effort of generating the surface and that of mobility calculation. The expense of both scales roughly linearly with the number of points defining the body, and that number is inversely proportional to the grid spacing cubed. By experience, a value of 0.1 Å or slightly less (depending on the ion size) is a reasonable compromise.[27] There are two contributions to the inaccuracy arising from the finiteness of grid spacing. The first is simply due to the finite number of "pixels" delimiting an image. The second (perhaps more insidious one) is because of the roughness introduced by the discretization of a smooth surface, which results in fictitious multiple reflections of buffer gas atoms. While the former error is statistical and thus random in nature, the latter is systematic as multiple collisions always elevate the cross section.[14] Consequently the grid spacing must be held constant for all systems, so that the errors due to induced surface roughness would cancel out in comparison. All results reported herein are for the 0.08 Å mesh size. Hence the isosurfaces contain thousands to tens of thousands of points, depending on the cluster size and shape.

The electron density isosurfaces used in this work have been constructed using DFT with the gradient-corrected functional Perdew−Wang−Becke 88. We have adopted the double numeric basis set with polarization functions as implemented in the all-electron DMOL code.[28] The value for electron density to delimit the surfaces has been adjusted to match the experimental room-temperature mobility of C_{60}^+ fullerene. This has produced $E_{cut} = 2.5 \times 10^{-3}$ (au)$^{-3}$, which is very close to the values of 2.6×10^{-3}−3.0×10^{-3} (au)$^{-3}$ obtained[27] by fitting the mobilities measured for Si_n^+ and Si_n^-. For both C and Si clusters, these values for E_{cut} have been obtained assuming a He radius (R_{He}) of 1.1 Å (the accepted van der Waals radius of He atom[8,29]). Variations of R_{He} obviously affect the values for E_{cut}; however, the final result for cross section is not influenced significantly as long as R_{He} is sensible. To visualize how a cluster geometry is viewed by different methods for mobility calculations, in Figure 1 we depict the C_{18}^+ monocyclic ring as it appears to the projection approximation, EHSS, and SEDI.

We have used SEDI to compute Ω for a representative set of carbon cluster ions belonging to the major structural families

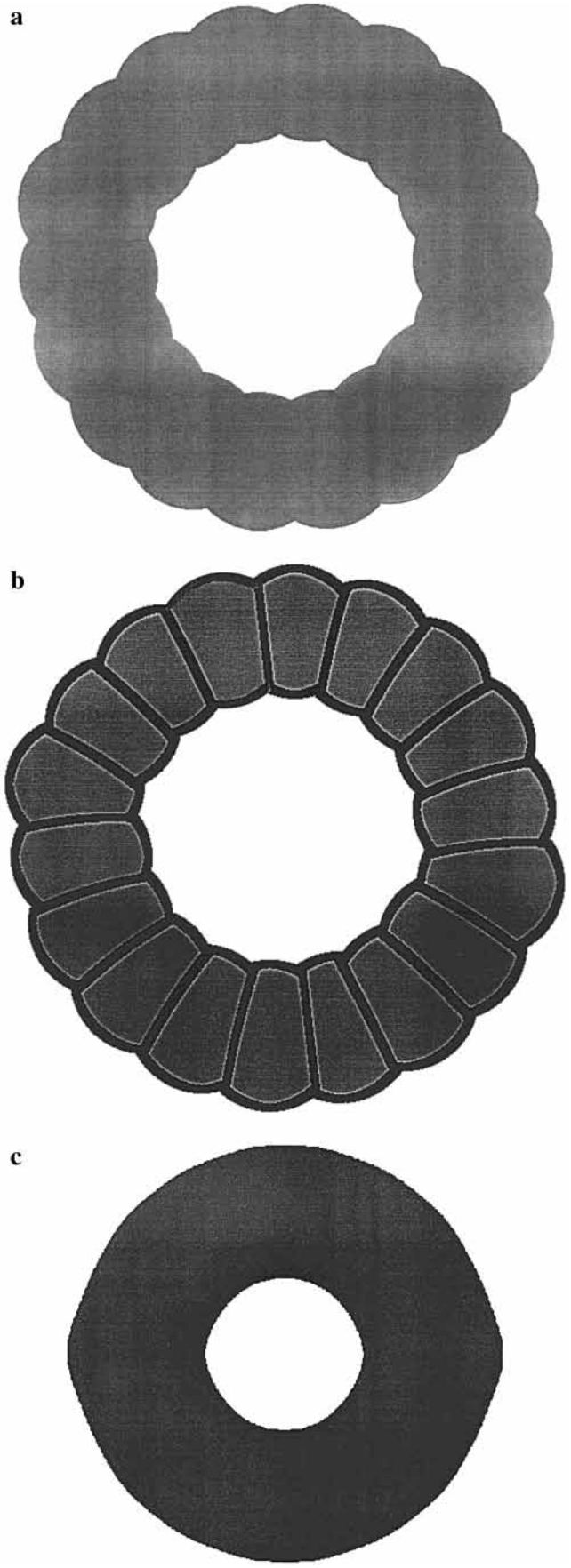

Figure 1. Representations of C_{18} ring cation by the projection approximation (a), exact hard-spheres scattering model (b), and scattering on electron density isosurfaces (c).

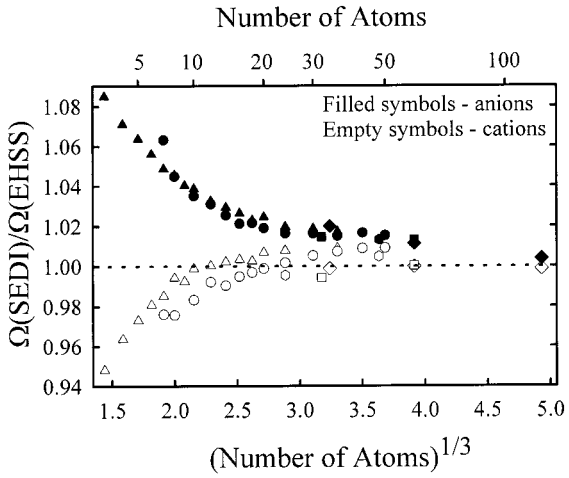

Figure 2. Collision integrals for carbon cluster cations and anions calculated using scattering on electron density isosurfaces relative to those determined by exact hard-spheres scattering model.[14] Examples displayed are representative of major C_n structural families: chains (triangles), monocyclic rings (circles), bicyclic rings (hexagons), graphite sheets (squares), and fullerenes (diamonds). We have included chain cations with $n > 10$ and ring anions with $n < 10$ that have not been observed experimentally in order to enable a comparison with the clusters of opposite charge actually found in mobility measurements.

encountered in mobility measurements. These are chains, monocyclic and bicyclic rings, graphite sheets, fullerenes, and fullerene dimers.[7−11,26,30−34] For cations, the size ranges of existence of these geometries are $n \leq 10$ for chains, $n \geq 7$ for monocyclic rings, $n \sim 20-40$ for bicyclic ones, $n \geq 29$ for graphite sheets, and $n \geq 30$ for fullerenes.[7,8,31,32] Fullerene dimers have been observed[9,10,15,33] for $n \sim 110-140$. The situation for anions is similar, except that chains persist[11] to $n \sim 50$ but monocyclic rings start at $n = 10$. Nuclear geometries adopted for these species are identical to those used in an extensive work on the application of trajectory calculations[11] to C_n^+. Briefly, linear chains and rotationally symmetric monocyclic ring isomers were assumed to have cumulenic bonding with 1.29 Å for all C−C bond lengths, and geometries for bicyclic rings, graphite sheets, and fullerenes were optimized using the MNDO semiempirical method.[35] While these geometries are somewhat imprecise (for example, in reality carbon rings have no rotational symmetry[36,37] and not all bonds in a carbon chain have the same length[38,39]), the resulting inaccuracy is slight and affects the mobilities calculated with any method systematically.

Collision integrals evaluated using SEDI are compared with EHSS values in Figure 2. (The C−He collision distance employed in EHSS, R_{C-He}, has likewise been fit to the measurement for C_{60}^+.) As one would expect, SEDI cross sections for anions are larger than EHSS values, the difference increasing for smaller clusters. This is a manifestation of greater electronic spill-out due to a stronger negative charge on a per-atom basis. The same behavior has been observed for Si_n anions.[27] Conversely, SEDI cross sections for small C_n^+ are lower than those obtained using EHSS because of the contraction of electronic orbitals pulled in by increasing average partial positive charge. For either charge state, the deviations from EHSS values are dependent mostly on the cluster size, with shape having but a minor role. It is interesting that SEDI cross sections for large ring and chain ions appear to converge to the values that slightly exceed those determined by EHSS. This may reflect the difference in extent of electronic orbitals between

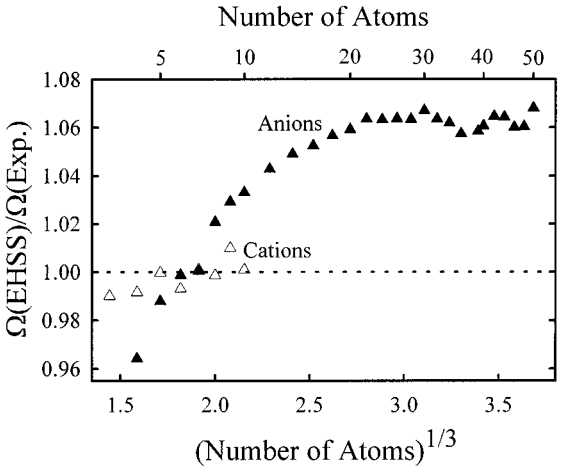

Figure 3. Collision integrals for carbon chain cations (empty symbols) and anions (filled symbols): values calculated using the exact hard-spheres scattering model (fit for $n = 7$ in both cases) versus the measurements.

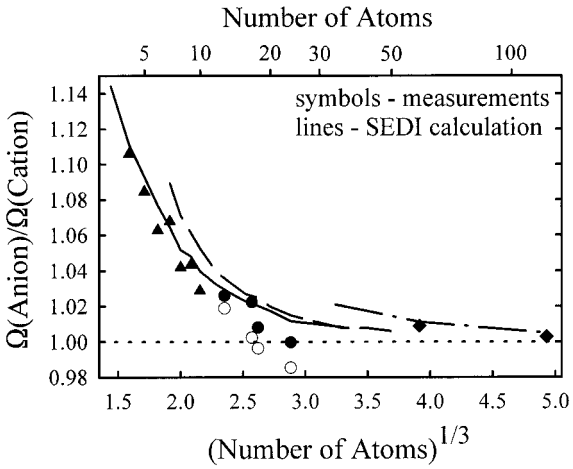

Figure 4. Collision cross sections for C_n anions belonging to various isomer families relative to those for cations. Representative measurements are marked by triangles for chains, circles for monocyclic rings, and diamonds for fullerenes. Filled and empty circles correspond to two different interpretations of the high-resolution measurements[22] for ring anions (see text). Lines result from scattering on electron density isosurfaces (solid line for chains, dashed for monocyclic rings, and dash−dot−dash for fullerenes). Fullerene dimers are omitted.

sp-carbons in rings and chains and sp^2-carbons in graphite sheets and fullerenes (recalling that the parameters of SEDI model were fit for C_{60}).

The contraction of electron cloud for Si_n cations has been found negligible in comparison with its expansion for anions.[27] It may seem via inspection of Figure 2 that this does not hold for carbon clusters other than fullerenes. However, it is well-known that the value of R_{C-He} fit for fullerenes is not transferable to C_n species belonging to other structural families.[7,11,29] Hence, to elucidate the true magnitudes of expansion or contraction of electron orbitals for non-fullerene carbon ions correctly, one has to reevaluate the C−He collision distance for those species. For example, the measurement for C_7^+ chain is fit assuming $R_{C-He} = 2.52$ Å (Figure 3). This value produces an excellent agreement with experimental mobilities for cationic chains of any length. The cross section measured for C_7 chain anion is larger than that for cation, so the appropriate value of R_{C-He} is greater, namely 2.64 Å. As exhibited in Figure 3, the mobilities for other chain anions calculated using EHSS with this value grossly disagree with the experiment. (This remains the case no matter for which size R_{C-He} is fit.) The same distinction between cations and anions exists for ring geometries. Hence the behavior of C_n ions in this regard is in fact similar to that of silicon species, and apparently is characteristic of clusters in general.

By inspection, surfaces of electron "isodenses" are smoother than those formed by spheres centered on atoms. A pertinent question is whether EHSS may systematically exaggerate the local surface roughness of polyatomic ions due to a finite atom size. This would bring about an overestimate of the number of multiple collisions with buffer gas atoms, which may cause an overvaluation of the collision integral.[14] To address this, we have calculated the orientationally averaged projections of electron density isosurfaces for C_n ions, applying

$$\Omega = \frac{1}{4\pi}\int_0^{2\pi} d\theta \int_0^{\pi} d\varphi \sin\varphi \int_0^{2\pi} d\gamma \int_0^{\infty} b\, db\, M(\theta,\varphi,\gamma,b) \quad (4)$$

where M is an integer-valued function that is unity when a hard-sphere collision occurs for a geometry defined by θ, φ, γ, b and null otherwise. Indeed, the differences between the computed collision integrals and projections for carbon clusters represented by electron clouds are smaller than those for the same species defined via nuclear coordinates. For example, for C_{120} T_d fullerene[40,41] this difference is 1.3% in the former case but 2.3% in the latter. A similar effect has been found for all carbon clusters regardless of shape. However, the values for Ω/P ratio obtained for electron density isosurfaces are still high estimates since they are elevated by artifactual surface roughness due to the finite grid spacing as described above. This means that the increase in cross section compared to projection induced by surface roughness should, in general, be less than that suggested by EHSS. This is particularly relevant for biological ions, where calculated Ω routinely exceeds the projection by ~20% and more.[19,20,42,43] The difference of this magnitude is highly significant for structural assignments, and this matter is a subject of our ongoing research.

III. Comparison of SEDI Mobilities with Measurements

We have mentioned that the major deficiency of trajectory calculations/EHSS is their inability to model the ionic mobility as a function of charge state. Therefore we first test the performance of SEDI in simulating the difference in cross sections between singly charged C_n anions and cations (Figure 4). Evidently, the method is quite successful in predicting the charge dependence of room-temperature mobilities measured for chains[11] and fullerenes.[9,10] For various C_{60} and C_{70} fullerene dimers with $n = 114-144$ (not plotted in Figure 4), the cross sections measured for anions exceed those for cations[10] by ≈1%. The value for [2+2] $(C_{60})_2$ cycloadduct calculated using SEDI is ≈1.2%. No comparison for graphite sheets could be made as no accurate data for anions are available.

The situation for rings is less straightforward. Recent high-resolution measurements[23] for C_n^- have revealed the splitting of monocyclic ring peak into two or more features for all $n \geq 13$. These have been assigned to "tadpoles" (rings with chains attached proposed earlier by theorists[44,45]), although the mobilities calculated for such geometries had not matched the experimental pattern well. When excited by a laser beam, all the above features seem to largely convert into peaks with the shortest drift times. Jarrold and co-workers[23] have interpreted this observation to suggest that those peaks are true monocyclic rings while other features are tadpoles. However, the cross sections of peaks with the shortest drift times (empty circles in

Figure 4) are significantly smaller than those expected for monocyclic ring anions. While SEDI calculations tend to exaggerate the difference between mobilities of anions and cations slightly, there is no rationale why the error for rings should be much greater than that for both smaller chains and larger fullerenes. Thus the apparent overvaluation of collision integrals for monocyclic ring anions in Figure 4 should be explained in terms of cluster geometries.

One possible reason is that tadpoles really exist for C_n cations in an abundance comparable to that for anions, but are hidden in low-resolution measurements under the single "monocyclic ring" peaks. If this is correct, the values reported for cross sections of some ring cations are then actually weighted averages over the true rings and one or more tadpoles. If the peaks at shortest drift times correspond to rings, the cross sections published for ring cations are overestimates. Unfortunately, no high-resolution measurements for cations that would determine this directly are presently available. However, we have convoluted the features observed for ring and tadpole anions with the low resolution of data for cations. This yields only one peak for each size. The mobilities of these peaks (filled circles in Figure 4) match the values calculated by SEDI. An alternative explanation is that the features with the shortest drift times are not necessarily due to true rings. Either way, one may conclude that the story with tadpole geometries for carbon clusters is still far from clear.

Similarly, high-resolution measurements for anions[23] have revealed multiple peaks in the bicyclic ring band. These features were believed[23] to correspond to different bicyclic ring geometries,[42,43] but may also be due to "bicyclic tadpoles" involving a chain attached to a bicyclic ring. The ambiguity of structural identities of these species makes it impossible to reliably evaluate the performance of SEDI for bicyclic rings.

IV. Formulation of the SEDI−TC Hybrid Model and Its Validation for Carbon Cluster Ions

In the previous section, we have demonstrated that the SEDI treatment correctly reproduces the difference between mobilities of C_n cations and anions of all sizes and shapes. It has, however, been expected (section I) that this model would fail to predict the absolute values. Indeed, the collision integrals for chain cations evaluated using SEDI agree with the measurements better than those determined by either the projection approximation or EHSS, but worse than those resulting from trajectory calculations (Figure 5). Clearly, the overestimation of cross sections for chains by the projection approximation, EHSS, and SEDI has one cause: all three methods ignore the long-range attractive potential explicitly. However, it is unavoidably included in the fitting of R_{C-He} (projection approximation, EHSS) or E_{cut} (SEDI) quantities that determine the expanse of effective hard walls. For geometries with relatively shallow molecular long-range potential such as chains, this overestimates the attractive interaction. Since trajectory calculations treat the attractive interactions explicitly, the change in their magnitude on going to chains is accounted for, hence a better agreement with experiment. It thus appears that a method depicting the repulsive interaction through electronic density, but still expressly introducing the attractive part of the potential, should be suitable for all kinds of ions.

Ideally, one would have to construct the potential energy surface for ion−He complex from first principles and evaluate the integral (4) by propagating trajectories on this surface. This extremely demanding approach has not been pursued yet. However, it may be possible to incorporate the long-range

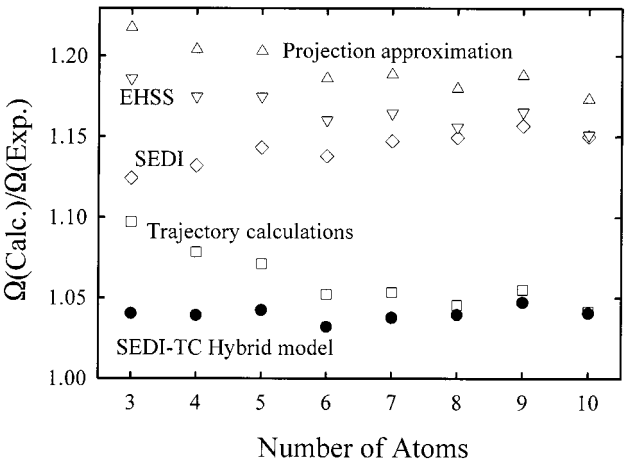

Figure 5. Collision integrals for C_n chain cations: theory versus experiment. Computed values are determined by projection approximation[11] (triangles up), exact hard-spheres scattering (triangles down), scattering on electron density isosurfaces (diamonds), trajectory calculations[11] (squares), and new hybrid treatment described in this contribution (circles). All models have been fit for C_{60} fullerene cation.

interactions approximately via a model coupling the scattering on electron density isosurfaces with traditional trajectory calculations in the additive pairwise Lennard-Jones potential. We set this hybrid SEDI−TC procedure up by factorizing the contribution from attractive interaction as a correction factor:

$$\Omega(\text{SEDI−TC}) = \Omega(\text{SEDI}) \times (\Omega(\text{trajectory calculations})/\Omega(\text{EHSS})) \quad (5)$$

The idea behind eq 5 is that the error inherent in the implicit estimation of that contribution in both EHSS and SEDI is approximately equal in the two methods. This mechanism modifies the SEDI value to roughly account for the strength of the attractive potential, or, from another viewpoint, amends the result of trajectory calculations to reflect the shape of the electron cloud.

Application of eq 5 with all three models customarily parameterized[13,14] for C_{60} cation to C_n^+ chains yields cross sections that systematically exceed the measurements at room temperature by ~4% (see Figure 5). This is materially superior to the performance of either trajectory calculations or SEDI alone for this system. It is also important that the error is size-independent and essentially equal to that for monocyclic carbon ring cations.[11] This suggests that the cause of the residual 4% discrepancy is simply the difference in interaction of He with sp-carbons in rings and chains on one hand and sp^2-carbons comprising graphite sheets and fullerenes on the other. It has already been pointed out[11] that, had the discrepancy between calculated and measured mobilities for chains indeed been caused by their bending motion, as suggested in some earlier work,[7,29] this discrepancy would have been steadily increasing with chain lengthening. As proven in section III, SEDI does a good job in modeling the relative mobilities of C_n^- and C_n^+ (Figure 4). Since in trajectory calculations or EHSS the results for these two charge states are nearly indistinguishable, the hybrid model of eq 5 would yield virtually the same relative mobilities as those given by SEDI. Hence the SEDI−TC model would also reproduce the absolute mobilities for carbon cluster anions, with a constant relative offset similar to that for cations in Figure 5. Of course, there is nothing magic about our choice of C_{60}^+ to parametrize eq 5, nor are the errors for chains plotted in Figure 5 physical themselves. It would be equally valid to adjust all compared models to fit the mobility measured for some

other species, for example a carbon chain, and evaluate the performance of each for fullerenes. The true quality gauge is the capability of a treatment to minimize discrepancies with experiment across the whole range of cluster sizes, shapes, and charge states.[11]

For Si_n cations and anions, Ω(trajectory calculations) $\approx$ Ω(EHSS) because of the unimportance of attractive potential (section I). Then by eq 5 Ω(SEDI−TC) = Ω(SEDI), which is in excellent agreement with the measurements for both cations and anions.[27] While the formalism (5) has transparent physical grounds and works well for carbon cluster ions, it still is a semiempirical treatment. Its general merit would eventually have to be assessed by comparison with a larger body of data.

V. Conclusions

A recently developed method to evaluate ionic mobilities by scattering on electron density isosurfaces (SEDI) has been applied to carbon cluster ions belonging to all major structural families. Cross sections calculated for anions exceed the values computed using the exact hard-spheres scattering model substantially because of the expansion of electron cloud. To the contrary, SEDI cross sections for cations deviate from the EHSS values only slightly. This behavior resembles that reported for Si_n ions. Relative mobilities of C_n^- and C_n^+ in He predicted by SEDI closely agree with the measurements for all cluster sizes and shapes considered. This agreement is substantially better than that found[27] for silicon species, particularly bearing in mind that it lasts over a much wider range of geometries and cluster sizes.

However, SEDI produces large errors in calculating the absolute mobilities for C_n ions of either charge. This has been expected as the long-range ion−He potential critical for correct evaluation of carbon cluster mobilities[11] is not involved. Hence we have developed a new SEDI−TC formalism that approximately couples the repulsive part of the overall interaction potential accurately simulated by SEDI with the attractive part accounted for via trajectory calculations. This hybrid model has been tested for C_n ions and has shown an excellent performance in calculating both relative and absolute mobilities for these species.

Acknowledgment. We are grateful to Professor David E. Clemmer, Professor Alan C. Hopkinson, and Professor Mark A. Ratner for many useful discussions on the scattering off electron clouds. We thank Dr. Gert von Helden, Dr. Thomas Wyttenbach, and Professor Michael T. Bowers for providing us their data on mobilities of carbon cluster ions. This research was supported by the National Science and Engineering Research Council of Canada, Canadian Foundation for Innovation, MDS Sciex, and the USDoE Office of Basic Energy Sciences.

References and Notes

(1) Hagen, D. F. *Anal. Chem.* **1979**, *51*, 871.
(2) Dugourd, Ph.; Hudgins, R. R.; Clemmer, D. E.; Jarrold, M. F. *Rev. Sci. Instrum.* **1997**, *68*, 1122.
(3) Jarrold, M. F. *J. Phys. Chem.* **1995**, *99*, 11.
(4) Mason, E. A.; McDaniel, E. W. *Transport Properties of Ions in Gases*; Wiley: New York, 1988.
(5) Hirschfelder, J. O.; Curtiss, C. F.; Bird, R. B. *Molecular Theory of Gases and Liquids*; Wiley: New York, 1964.
(6) Mack, Jr., E. *J. Am. Chem. Soc*. **1925**, *47*, 2468.
(7) von Helden, G.; Hsu, M. T.; Gotts, N. G.; Bowers, M. T. *J. Phys. Chem.* **1993**, *97*, 8182.
(8) von Helden, G.; Hsu, M. T.; Gotts, N. G.; Kemper, P. R.; Bowers, M. T. *Chem. Phys. Lett.* **1993**, *204*, 15.
(9) Shvartsburg, A. A.; Hudgins, R. R.; Dugourd, Ph.; Jarrold, M. F. *J. Phys. Chem. A* **1997**, *101*, 1684.
(10) Shvartsburg, A. A.; Hudgins, R. R.; Gutierrez, R.; Jungnickel, G.; Frauenheim, T.; Jackson, K. A.; Jarrold, M. F. *J. Phys. Chem. A* **1999**, *103*, 5275.
(11) Shvartsburg, A. A.; Schatz, G. C.; Jarrold, M. F. *J. Chem. Phys*. **1998**, *108*, 2416.
(12) Liu, B.; Lu, Z. Y.; Pan, B. C.; Wang, C. Z.; Ho, K. M.; Shvartsburg, A. A.; Jarrold, M. F. *J. Chem.* Phys. **1998**, *109*, 9401.
(13) Mesleh, M. F.; Hunter, J. M.; Shvartsburg, A. A.; Schatz, G. C.; Jarrold, M. F. *J. Phys. Chem*. **1996**, *100*, 16082; *J. Phys. Chem. A* **1997**, *101*, 968.
(14) Shvartsburg, A. A.; Jarrold, M. F. *Chem. Phys. Lett*. **1996**, *261*, 86.
(15) Shvartsburg, A. A.; Pederson, L. A.; Hudgins, R. R.; Schatz, G. C.; Jarrold, M. F. *J. Phys. Chem.* A **1998**, *102*, 7919.
(16) Shvartsburg, A. A.; Liu, B.; Lu, Z. Y.; Wang, C. Z.; Jarrold, M. F.; Ho, K. M. *Phys. Rev. Lett*. **1999**, *81*, 4616.
(17) Dugourd, Ph.; Hudgins, R. R.; Jarrold, M. F. *Chem. Phys. Lett*. **1997**, *267*, 186.
(18) Doye, J. P. K.; Wales, D. J. *Phys. Rev. B* **1999**, *59*, 2292.
(19) Clemmer, D. E.; Jarrold, M. F. *J. Mass Spectrom*. **1997**, *32*, 577.
(20) Shelimov, K. B.; Clemmer, D. E.; Hudgins, R. R.; Jarrold, M. F. *J. Am. Chem. Soc*. **1997**, *119*, 2240.
(21) Gotts, N. G.; von Helden, G.; Bowers, M. T. *Int. J. Mass Spectrom. Ion Processes* **1995**, *149/150*, 217.
(22) Hudgins, R. R.; Dugourd, Ph.; Tenenbaum, J. M.; Jarrold, M. F. *Phys. Rev. Lett*. **1997**, *78*, 4213.
(23) Dugourd, Ph.; Hudgins, R. R.; Tenenbaum, J.; Jarrold, M. F. *Phys. Rev. Lett*. **1998**, *80*, 4197.
(24) Lerme, J.; Dugourd, Ph.; Hudgins, R. R.; Jarrold, M. F. *Chem. Phys. Lett.* **1999**, *304*, 19.
(25) Hudgins, R. R.; Imai, M.; Jarrold, M. F.; Dugourd, Ph. *J. Chem. Phys*. **1999**, *111*, 7865.
(26) von Helden, G.; Kemper, P. R.; Gotts, N. G.; Bowers, M. T. *Science* **1993,** *259*, 1300.
(27) Shvartsburg, A. A.; Liu, B.; Jarrold, M. F.; Ho, K. M. *J. Chem. Phys.* **2000**, *112*, 4517.
(28) DMOL package, 96.0/4.0.0; MSI, San Diego, 1996.
(29) von Helden, G.; Porter, E.; Gotts, N. G.; Bowers, M. T. *J. Phys. Chem*. **1995**, *99*, 7707.
(30) von Helden, G.; Hsu, M. T.; Kemper, P. R.; Bowers, M. T. *J. Chem. Phys*. **1991**, *95*, 3835.
(31) von Helden, G.; Gotts, N. G.; Palke, W. E.; Bowers, M. T. *Int. J. Mass Spectrom. Ion Processes* **1994**, *138*, 33.
(32) Shelimov, K. B.; Hunter, J. M.; Jarrold, M. F. *Int. J. Mass Spectrom. Ion Processes* **1994**, *138*, 17.
(33) Hunter, J. M.; Fye, J. L.; Boivin, N. M.; Jarrold, M. F. *J. Phys. Chem*. **1994**, *98*, 7440.
(34) Hunter, J. M.; Jarrold, M. F. *J. Am. Chem. Soc*. **1995**, *117*, 10317.
(35) The coordinates obtained by MNDO calculations were scaled by 0.9884. This is necessary to bring the MNDO geometry of C_{60} in agreement with experiment.[13]
(36) Martin, J. M. L.; El-Yazal, J.; Francois, J. P. *Chem. Phys. Lett*. **1996**, *252*, 9.
(37) Martin, J. M. L.; Taylor, P. R. *J. Phys. Chem*. **1996**, *100*, 6047.
(38) Raghavachari, K.; Strout, D. L.; Odom, G. K.; Scuseria, G. E.; Pople, J. A.; Johnson, B. G.; Gill, P. M. W. *Chem. Phys. Lett*. **1993**, *214*, 357.
(39) Martin, J. M. L.; El-Yazal, J.; Francois, J. P. *Chem. Phys. Lett*. **1996**, *255*, 7.
(40) Strout, D. L.; Murry, R. L.; Xu, C.; Eckhoff, W. C.; Odom, G. K.; Scuseria, G. E. *Chem. Phys. Lett*. **1993**, *214*, 576.
(41) Scuseria, G. E. In *Buckminsterfullerenes*; Billups, W. E., Ciufolini, M. A., Eds.; VCH: Weinheim, 1993; p 103.
(42) Chen, Y. L.; Collings, B. A.; Douglas, D. J. *J. Am. Soc. Mass Spectrom*. **1997**, *8*, 681.
(43) Counterman, A. E.; Valentine, S. J.; Srebalus, C. A.; Henderson, S. C.; Hoaglund, C. S.; Clemmer, D. E. *J. Am. Soc. Mass Spectrom*. **1998**, *9*, 743.
(44) Strout, D. L.; Book, L. D.; Millam, J. M.; Xu, C.; Scuseria, G. E. *J. Phys. Chem*. **1994**, *98*, 8622.
(45) Aleksandrov, A. L.; Bedanov, V. M.; Morokov, Y. N.; Shveigert, V. A. *J. Struct. Chem*. **1995**, *36*, 906.